

07.2

## Numerical modelling of aluminum distribution profiles in the Al–Ga–As–Sn epitaxial layer

© N.S. Potapovich, V.P. Khvostikov, O.A. Khvostikova, A.S. Vlasov

Ioffe Institute, St. Petersburg, Russia  
E-mail: nspotapovich@mail.ioffe.ru

Received September 7, 2023

Revised October 11, 2023

Accepted October 13, 2023

In this work, we simulated the concentration profiles of *nn*-AlGaAs layers doped with tin during growth by liquid-phase epitaxy from a melt of limited height. The possibility of obtaining thick gradient waveguide layers from melts with different tin content is shown. The influence of the solvent composition on the effect of aluminum profile gradient inversion has been studied.

**Keywords:** AlGaAs, phase equilibrium, liquid phase epitaxy, photovoltaic cells.

DOI: 10.61011/TPL.2024.01.57830.19721

It is known that in systems where solid solutions are formed by substitution of gallium by aluminium, high values of the aluminium distribution coefficient are observed. This property allows to obtain AlGaAs solid solutions at sufficiently low temperatures in a wide range of compositions. Such heterostructures allow to obtain rather thick layers (more than 40  $\mu\text{m}$ ) with a significant composition gradient or, on the contrary, homogeneous layers throughout the thickness, used in LEDs and photovoltaic converters with vertical *p*–*n*-junction. When creating devices based on thick AlGaAs layers (both homogeneous and gradient layers) grown in a wide range of temperatures, it is also necessary to solve the problem of obtaining homogeneous by level and type of doping of the layers. Thus, growth from gallium melt can lead to AlGaAs layers of both *n*-type and *p*-type. At a growth temperature of more 850°C, AlGaAs layers have *p*-type of conductivity, and at  $T < 850^\circ\text{C}$  — *n*-type [1,2]. Growth from tin-enriched melts allows to reliably obtain *n*-AlGaAs structures at high epitaxy temperatures (more than 850°C), but significantly shifts phase equilibria and consequently changes the profile of composition distribution along the thickness of the obtained layer.

The growth of epitaxial layers by liquid-phase epitaxy from a limited volume melt was modelled using the Pfann [3] equation. Substituting  $X_{\text{Al}}^S = X_{\text{AlAs}}/2$  and  $X_{\text{As}}^S = 1$  [4,5] into this equation, we can represent it as a differential equation with initial conditions  $X_{\text{Al}}^L = X_{\text{Al}0}^L$  at  $T = T_0$ :

$$dX_{\text{Al}}^L/dT = dX_{\text{As}}^L/dT [(0.5X_{\text{AlAs}} - X_{\text{Al}}^L)/(1 - X_{\text{As}}^L)], \quad (1)$$

where  $X_{\text{AlAs}}$  — aluminium content in the solid phase,  $X_{\text{As}}^L$  and  $X_{\text{Al}}^L$  — arsenic and aluminium content in the liquid phase.

The differential equation parameters ( $X_{\text{AlAs}}$ ,  $X_{\text{As}}^L$  and  $dX_{\text{As}}^L/dT$ ) were determined from the liquidus and solidus curves calculated using the quasi-regular solutions model for

$T = 1000\text{--}500^\circ\text{C}$  using the equations given in [6,7]. Equation (1) was integrated using the fourth-order Runge–Kutt method with a temperature step of 0.1°C.

Gradient AlGaAs layers were grown by liquid-phase epitaxy from Ga–Sn melt with a tin content of 0.2 mol. fraction. The growing layer was crystallized on GaAs substrates of orientation (100) in a stream of purified hydrogen. The epitaxial growth of layers was carried out in a piston-type graphite cassette with limited melt height ( $h = 1.5\text{ mm}$ ). The cooling rate of the solution-melt during epitaxy did not exceed 1°C/min. The epitaxial growth onset temperature was  $T_0 = 935^\circ\text{C}$  at an initial solid phase aluminium content of  $X_{\text{AlAs}0} = 0.58$  for the first sample (Fig. 1, *a*, curve 2, circles) and  $X_{\text{AlAs}0} = 0.53$  for the second sample (Fig. 1, *a*, curve 2, squares). The growth termination temperature and layer thickness for the first sample were 860°C and 40  $\mu\text{m}$ , and for the second sample — 800°C and 80  $\mu\text{m}$ , respectively.

The experimental values of the  $X_{\text{AlAs}}$  composition of the AlGaAs solid solution were determined using Raman-scattering spectroscopy. The spectra were measured in the geometry of backscattering from the end. Excitation was performed with a laser with an emission wavelength of 532 nm through an 80 $\times$  magnification lens.

As can be seen from Fig. 1, *a*, the general character of the composition distribution along the thickness of the AlGaAs epitaxial layer during epitaxial growth from Ga–Sn melt (Sn concentration is 0.2 mol. fraction) retains the appearance typical for growth from melts with gallium substitution by aluminium. In this case, the inversion of the aluminium profile gradient (increase in the aluminium content in the solid solution during growth instead of a decrease) of is also preserved because the decrease in the amount of nonmetal in the liquid phase is accompanied by an increase in the aluminium distribution coefficient upon cooling of the growth solution-melt [5,8]. The curve 1 in Fig. 1, *a* (inverse curve) indicates the change of aluminium profile gradient

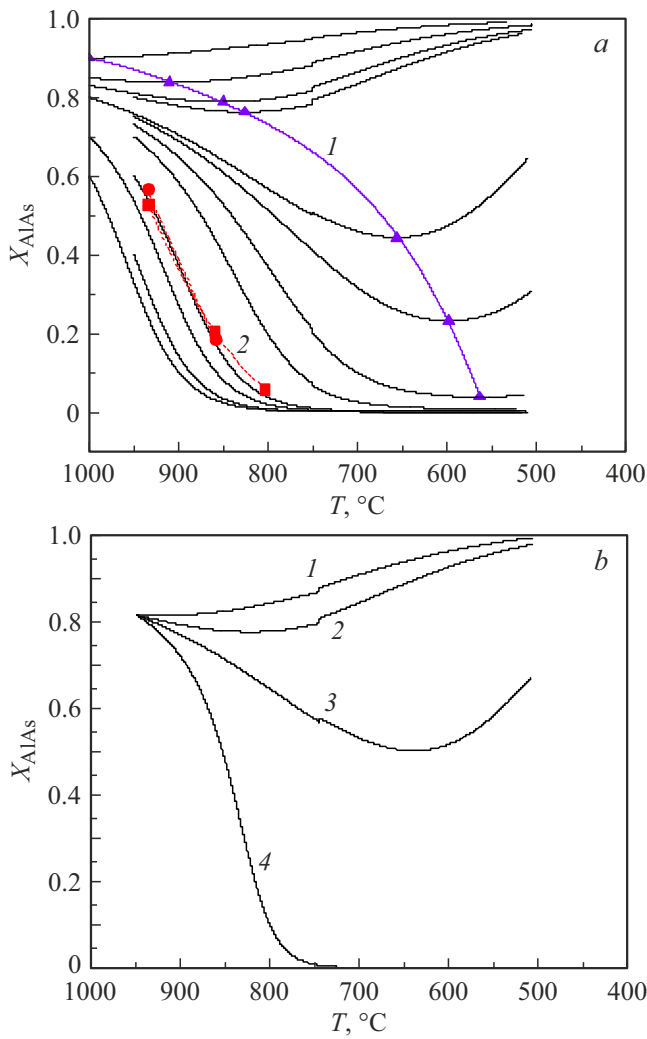


**Figure 1.** Change in the composition of AlGaAs epitaxial layer during growth from Ga-Sn melt. *a* — at Sn concentration equal to 0.2 mol. fraction (*1* — inverse curve, *2* — experimental profiles); *b* — at initial conditions ( $T_0 = 950^\circ\text{C}$ ,  $X_{AlAs0} = 0.8$ ) and tin concentration  $X_{Sn} = 0$  (*1*), 0.2 (*2*), 0.3 (*3*) and 0.4 mol. fraction (*4*).

during epitaxial growth. The obtained distribution profiles in the experimental samples (points and curves 2 in Fig. 1, *a*) agree quite well with the theory. Some discrepancies in the region of low aluminium concentrations ( $X_{AlAs} < 0.2$ ) may be due to the high error of the study method in this region of compositions.

Addition of tin to the growth melt already in the amount of 0.4 mol. fraction leads to a change in the character of solid solution composition distribution. In accordance with the calculation results shown in Fig. 1, *b*, when growing AlGaAs layers from Ga-Sn melt (under initial conditions  $T_0 = 950^\circ\text{C}$ ,  $X_{AlAs0} = 0.8$ ), changing the tin concentration, it is possible to achieve the growth of both layers with increasing aluminium content and gradient layers with decreasing aluminium content (up to the growth of GaAs layer).

The task of obtaining a gradient waveguide layer with a smooth change in the composition of *n*-type conductivity without sharp jumps in the doping level throughout the thickness (at least  $40\ \mu\text{m}$ ) may require sequential growth from several melts with different concentrations of donor impurity [2]. The inversion boundary of the aluminium profile gradient should be clearly monitored. Based on the results of modelling the changes in the composition of the AlGaAs epitaxial layer during epitaxial growth with different tin concentration in the melt ( $X_{Sn} = 0-0.4$  mol. fraction) inverse curves were determined (Fig. 2). For clarity, the region 4 corresponding to the compositions and temperatures most suitable for growing thick ( $d > 40\ \mu\text{m}$ ) AlGaAs gradient layers is shown in the figure.

As can be seen, in the case of growth from the melt with tin content less than 0.2 mol. fraction, it is possible to get into the region of inverse growth of AlGaAs (where the composition of the solid solution increases rather than decreases with decreasing temperature), which should be taken into account when planning experiments. Based on these studies, high-power photovoltaic converters with vertical *p-n*-junction, GaAs active region and thick waveguide layer  $\text{Al}_x\text{Ga}_{1-x}\text{As}$  ( $d \approx 50\ \mu\text{m}$ ), grown by liquid-phase epitaxy were obtained and investigated in [9,10].

Thus, in this work, the growth of gradient layers in the Al-Ga-As-Sn system has been modelled for different tin content in the melt. The possibility of applying the proposed calculation method for the growth of relatively thick layers ( $d > 40\ \mu\text{m}$ ) AlGaAs with a composition gradient or homogeneous over the entire thickness has been experimentally confirmed. A change in the inversion curves of the aluminium profile gradient when tin is added to the melt up to 0.4 mol. fraction has been determined and a shift of the inversion boundary to the region with higher aluminium content in the solid layer is shown. The obtained

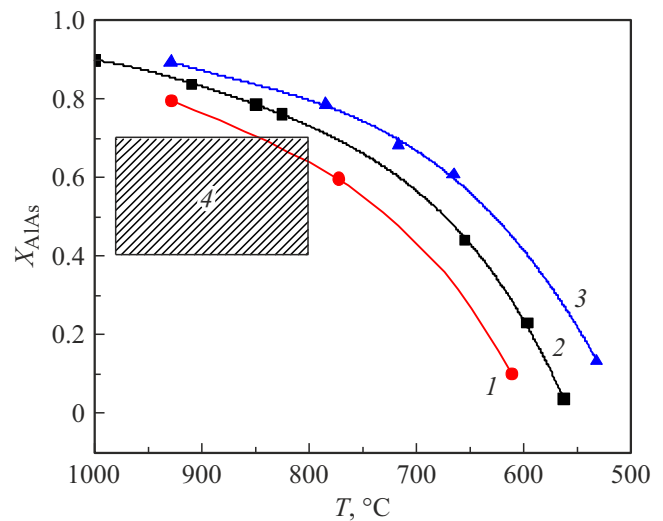


**Figure 2.** Inverse curves at different tin contents in the solution-melt.  $X_{Sn} = 0$  (*1*), 0.2 (*2*) and 0.4 mol. fraction (*3*). The region 4 — initial compositions and temperatures used for the growth of AlGaAs gradient layers.

results can be used to design photovoltaic converters with vertical  $p-n$ -junction.

### Funding

This study was supported by a grant from the Russian Science Foundation № 22-19-00057 (<https://rscf.ru/project/22-19-00057/>).

### Conflict of interest

The authors declare that they have no conflict of interest.

### References

- [1] X. Zhao, K.H. Montgomery, J.M. Woodall, J. Electron. Mater., **43** (11), 3999 (2014). DOI: 10.1007/s11664-014-3340-x
- [2] V. Khvostikov, O. Khvostikova, N. Potapovich, A. Vlasov, R. Sali, Heliyon, **9** (7), e18063 (2023). DOI: 10.1016/j.heliyon.2023.e18063
- [3] W.G. Pfann, *Zone melting* (Wiley, 1958). DOI: 10.1107/S0365110X5900130X
- [4] V.M. Andreev, L.M. Dolginov, D.N. Tretiakov, *Zhidkostnaya epitaksiya v tekhnologii poluprovodnikovyykh priborov* (Sov. Radio, M., 1975). (In Russian).
- [5] V.A. Elyukhin, S.Yu. Karpov, E.L. Portnoy, D.N. Tretiakov, Pisma v ZhTF, **4** (11), 629 (1978).
- [6] M.B. Panish, J. Appl. Phys., **44** (6), 2667 (1973). DOI: 10.1063/1.1662631
- [7] H.C. Casey, M.B. Panish, *Heterostructure lasers* (Academic Press, 1978), pt B, ch. 6. DOI: 10.1016/B978-0-12-163102-4.50009-9.
- [8] M. Dombrougov, Microsyst. Electron. Acoust., **24** (1), 6 (2019). DOI: 10.20535/2523-4455.2019.24.1.160164
- [9] A. Panchak, V. Khvostikov, P. Pokrovskiy, Opt. Laser Technol., **136**, 106735 (2021). DOI: 10.1016/j.optlastec.2020.106735
- [10] V.P. Khvostikov, A.N. Panchak, O.A. Khvostikova, P.V. Pokrovskiy, IEEE Electron Dev. Lett., **43** (10), 1717 (2022). DOI: 10.1109/LED.2022.3202987

*Translated by J.Deineka*